



**CHALMERS**  
UNIVERSITY OF TECHNOLOGY

## **Phenotypic and transcriptomic acclimation of the green microalga *Raphidocelis subcapitata* to high environmental levels of the herbicide**

Downloaded from: <https://research.chalmers.se>, 2024-03-20 09:08 UTC

Citation for the original published paper (version of record):

Gómez-Martínez, D., Bengtson, J., Nilsson, A. et al (2023). Phenotypic and transcriptomic acclimation of the green microalga *Raphidocelis subcapitata* to high environmental levels of the herbicide diflufenican. *Science of the Total Environment*, 875. <http://dx.doi.org/10.1016/j.scitotenv.2023.162604>

N.B. When citing this work, cite the original published paper.



# Phenotypic and transcriptomic acclimation of the green microalga *Raphidocelis subcapitata* to high environmental levels of the herbicide diflufenican

Daniela Gómez-Martínez<sup>a,\*</sup>, Johanna Bengtson<sup>a</sup>, Anders K. Nilsson<sup>b</sup>, Adrian K. Clarke<sup>a</sup>, Rolf Henrik Nilsson<sup>a</sup>, Erik Kristiansson<sup>c</sup>, Natàlia Corcoll<sup>a,\*</sup>

<sup>a</sup> Department of Biological and Environmental Sciences, University of Gothenburg, Gothenburg, Sweden

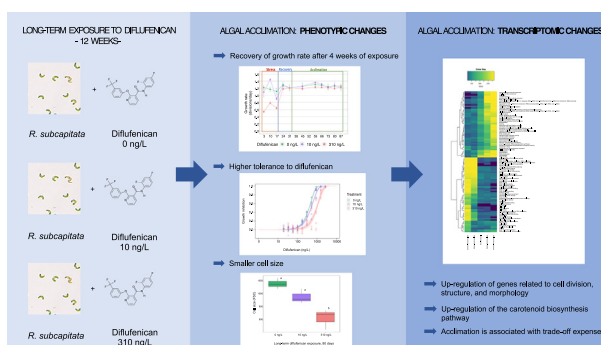
<sup>b</sup> Department of Clinical Neuroscience, Institute of Neuroscience and Physiology, Sahlgrenska Academy, University of Gothenburg, Gothenburg, Sweden

<sup>c</sup> Department of Mathematical Sciences, Chalmers University of Technology and University of Gothenburg, Gothenburg, Sweden

## HIGHLIGHTS

- Phenotypic and transcriptomic analysis were applied to study the acclimation of *Raphidocelis subcapitata* towards the herbicide diflufenican.
- *R. subcapitata* was able to acclimate to toxic environmental concentrations of the herbicide diflufenican after one month of exposure.
- Trade-off expenses of tolerance induction resulted in a reduction in cell size.
- Gene sets related to cellular division, DNA repair and replication, and protein folding were up-regulated as a result of acclimation to diflufenican.

## GRAPHICAL ABSTRACT



## ARTICLE INFO

Editor: Frederic Coulon

**Keywords:**  
Acclimation  
Microalgae  
Transcriptomics  
Diflufenican  
Carotenoids

## ABSTRACT

Herbicide pollution poses a worldwide threat to plants and freshwater ecosystems. However, the understanding of how organisms develop tolerance to these chemicals and the associated trade-off expenses are largely unknown. This study aims to investigate the physiological and transcriptional mechanisms underlying the acclimation of the green microalgal model species *Raphidocelis subcapitata* (Selenastraceae) towards the herbicide diflufenican, and the fitness costs associated with tolerance development. Algae were exposed for 12 weeks (corresponding to 100 generations) to diflufenican at the two environmental concentrations 10 and 310 ng/L. The monitoring of growth, pigment composition, and photosynthetic performance throughout the experiment revealed an initial dose-dependent stress phase (week 1) with an EC<sub>50</sub> of 397 ng/L, followed by a time-dependent recovery phase during weeks 2 to 4. After week 4, *R. subcapitata* was acclimated to diflufenican exposure with a similar growth rate, content of carotenoids, and photosynthetic performance as the unexposed control algae. This acclimation state of the algae was explored in terms of tolerance acquisition, changes in the fatty acids composition, diflufenican removal rate, cell size, and changes in mRNA gene expression profile, revealing potential fitness costs associated with acclimation, such as up-regulation of genes related to cell division, structure, morphology, and reduction of cell size. Overall, this study demonstrates that *R. subcapitata* can quickly acclimate to environmental but toxic levels of diflufenican; however, the acclimation is associated with trade-off expenses that result in smaller cell size.

\* Corresponding authors.

E-mail addresses: [daniela.gomez.martinez@bioenv.gu.se](mailto:daniela.gomez.martinez@bioenv.gu.se) (D. Gómez-Martínez), [natalia.corcoll@bioenv.gu.se](mailto:natalia.corcoll@bioenv.gu.se) (N. Corcoll).

## 1. Introduction

Diffenfenican is a fluorinated herbicide commonly used in the agricultural sector in Europe due to its high efficacy to reduce broadleaf weeds in winter cereal crops (Messelhäuser et al., 2021). Diffenfenican residues are detected in many European surface waters nearby agricultural activities. For instance, in Swedish rivers and streams, concentrations of diffenfenican can range between 10 to 100 ng/L (Boye et al., 2019), and up to 503 ng/L in Spanish rivers (Herrero-Hernández et al., 2020), being in many cases above the predicted non-effect concentrations (PNEC) for the environment (4.5 ng/L; Boström et al., 2017). The derived ecological risk of diffenfenican in water bodies is mainly due to its high toxicity to algae, with an EC<sub>50</sub> value (72 h) ranging from 270 to 510 ng/L (Book et al., 2022; Weyman et al., 2012). Diffenfenican is currently included in the watch list of substances for the European Union-wide monitoring in the field of water quality (EU Directive 2008/105/EC).

Diffenfenican acts by blocking the biosynthesis of the carotenoid pigments (Miras-Moreno et al., 2019), which starts with the condensation of two geranylgeranyl diphosphate (GGPPs) to produce phytoene, and in turn, is transformed to lycopene through the action of the phytoene desaturase (PDS). Diffenfenican specifically blocks the desaturation step by inhibiting the PDS activity, thereby impeding the entire carotenoid biosynthetic pathway. The lack of carotenoid pigments typically results in the death of the whole plant, due to the fundamental importance of this pigments' family in the dissipation of excess excitation energy during photosynthesis (Miras-Moreno et al., 2019).

Microalgae comprise a diverse functional group of eukaryotic photosynthetic organisms that occupy nearly every aquatic environment (Wu et al., 2017). Through photosynthesis, algae use light energy to fix carbon dioxide into complex organic molecules that act as the main carbon source for organisms occupying higher trophic levels (Ramaraj et al., 2014). Due to their importance, ubiquity, and strong sensitivity to environmental changes, microalgae are commonly used as standard tests organisms in bioassays, representing an efficient and fundamental approach in the evaluation of the ecological risk and toxicity of chemicals that are released into surface waters (Ceschin et al., 2021; Wu et al., 2017). The globally distributed green microalga *Raphidocelis subcapitata* (Selenastraceae; syn. *Pseudokirchneriella subcapitata*) is regularly used as a model species for standard ecotoxicological growth assays (OECD 201). As a result, a detailed ecotoxicological dataset based on the effective median concentration (EC<sub>50</sub>) of this species has been built up over the years. However, this knowledge is restricted to growth tests, where the species is exposed to a compound for a period of 72 to 96 h (OECD 201). Scarce information is available on how *R. subcapitata* responds during longer exposure times. Previous studies have shown that algae possess a great phenotypic plasticity to acclimate towards chemical stressors such as heavy metals via changes in gene expression (Thiriet-Rupert et al., 2021).

From an environmental perspective, herbicide sub-lethal effects and acclimation mechanisms would be more expected rather than lethal effects, since lethal concentrations are rarely reached in freshwater environments (Huertas et al., 2010). The acclimation processes imply fitness trade-offs due to the changes in the allocation of energy resources, resulting in a loss of fitness in cellular functions not directly related to responses to the stressor (Yoshida et al., 2004). Hence, it is important that we identify effects and acclimation mechanisms towards hazardous chemicals at sub-lethal levels, and that we improve our understanding of the biological expenses of acclimation. Gene expression-based studies of acclimation processes in microalgal model species to potentially harmful substances in environmental concentrations – that is, of ecotoxicological relevance – are scarce.

In this study, we aimed to investigate via an acclimation laboratory experiment the ability of *R. subcapitata* to acclimate to two environmental concentrations of diffenfenican — one low (10 ng/L) and another close to the EC<sub>50</sub> based on growth rate after 72 h (310 ng/L) over an ecological timescale of 12 weeks. We examined the physiological and molecular mechanisms underlying the algal acclimation and associated fitness costs by measuring changes in growth rate, pigment content, tolerance

induction, cell size, fatty acids composition and content, as well as gene expression via mRNA-sequencing analysis.

## 2. Materials and methods

### 2.1. Experimental design

The experimental design included unexposed controls and two diffenfenican exposures (10 and 310 ng/L), each in triplicate flasks. Both tested concentrations of the herbicide were environmentally relevant based on previous studies (Boye et al., 2019; Herrero-Hernández et al., 2020). The higher tested concentration is close to the EC<sub>50</sub> for *R. subcapitata* based on growth rate (previously determined in our lab EC<sub>50</sub> 72 h = 397 ng/L). All replicates were sourced from the same batch culture. Each replicate (n = 3 per test concentration), was cultivated in 260 mL Nunc™ Non-treated Flasks (Thermo Scientific™, cat n° 132903) with an initial density of 20,000 cells/mL, in 50 mL of C medium (Ichimura, 1971) spiked with the corresponding test concentrations of diffenfenican (see below). Cultures were maintained throughout the experiment under axenic conditions, using an adjusted serial batch culture approach of LaPanse et al. (2021), by harvesting the cells in the late exponential growth phase and re-inoculating them in fresh media containing diffenfenican (including 10 or 310 ng/L diffenfenican for the treated cultures) every week at a starting cell density of 20,000 cells/mL.

Algal re-inoculation was performed by taking the corresponding volume from the 7-day-old cultures to have a final concentration of ~20,000 cells/mL in 6 mL of medium C. Next, 5 mL of each algal diluted culture was diluted onto 45 mL of fresh media to form a working volume of 50 mL in each flask.

Cell growth and photosynthetic performance (as determined by the maximum quantum yield of photochemical energy conversion in photosystem II [PSII]) were measured once a week (after 72 h when cells were in exponential growth and after 7 days of re-inoculation, respectively). Samples for pigment profiling were taken weekly. However, samples corresponding to weeks 5, 6 and 8 were lost due to technical problems. At the end of the experiment (week 12), samples for fatty acids composition and cell size analysis as well as mRNA sequencing were taken for all test concentrations after 72 h of re-inoculation (exponential phase).

### 2.2. Study species and culture conditions

The green microalga *Raphidocelis subcapitata* was used in the present study. A clonal and axenic strain of *R. subcapitata* NIES-35 (= ATCC22662) was purchased from the Microbial Culture Collection at the National Institute for Environmental Studies, Japan (<http://mcc.nies.go.jp>). The strain was cultivated in 50 mL flasks (Nunc™ Non-treated Flasks, Thermo Scientific™) containing medium C (Ichimura, 1971) and grown in a phytotron chamber at 21 ± 2 °C under daylight fluorescence tubes (~100 μmol photons/m<sup>2</sup>/s) with a 16 h photoperiod cycles. Cultures were constantly agitated using a horizontal shaker set to 55 rpm. The culture cell densities were measured by chlorophyll-a fluorescence (VarioskanFlash version 4.00.53) using 250 μL aliquots in 96 well-plates (Supplementary material), with the accuracy of the measurements confirmed by flow cytometry (CyFlow® Cube 8 flowcytometer, Sysmex Partec GmbH, Görlitz, Germany).

Prior to the experiment, growth was monitored for 10 days in 24 h intervals to establish the lag (2 d), exponential (3 d), stationary (2 d) and decline (2 days)-phases of NIES-35 under our test system. Starting cell density was ca. 20,000 cells/mL. A batch culture was produced 72 h prior to the start of the experiment in 260 mL flasks (Nunc™ Non-treated Flasks (Thermo Scientific™, cat n° 1329039) to ensure enough cells in the exponential-growth phase.

### 2.3. Diffenfenican stocks and tests

To obtain the different test concentrations, one diffenfenican stock solution (27.5 mg/L in 96 % MeOH) was prepared from powdered diffenfenican (CAS nr 83164-33-4; Sigma-Aldrich, Merck KGaA). From this solution, an

intermediate solution of 6.42 mg/L was prepared fresh for every new inoculation (weekly). Briefly, 28.8  $\mu$ L of diflufenican stock solution (27.5 mg/L) were pipetted into 50 mL sterile centrifuge tubes. After MeOH evaporation, 40 mL of sterile C medium was added and rigorously shaken in the dark for 1 h, allowing the diflufenican to mix well. The intermediate diflufenican solution was vortexed for a further 3 min and then used to prepare the different diflufenican test concentrations (i.e., 0, 10 and 310 ng/L) in 500 mL sterile glass Erlenmeyer flasks filled with sterile medium C up to 160 mL. Flasks were shaken again by hand for another 5 min. A total of 45 mL of each solution were placed in the culture flasks before algal re-inoculation. This procedure was repeated weekly for the entire duration of the experiment.

Non-algae control flasks were also prepared in the same way as the flasks containing algae (i.e., three different concentrations of diflufenican and in triplicates) to monitor the potential abiotic loss of diflufenican.

## 2.4. Phenotypic descriptors

### 2.4.1. Growth rate

The growth rate of cultures was calculated using the equation provided by Chalifour and Tam (2016):

$$\mu \text{ (days}^{-1}\text{)} = \frac{\ln N_x - \ln N_0}{t_x - t_0}$$

where  $N_x$  and  $N_0$  are the chlorophyll-*a* fluorescence values at day *X* and 0, respectively, and  $t_x$  and  $t_0$  are the corresponding sampling time points.

### 2.4.2. Cell size

Cell size data was collected using a flow cytometer (CyFlow® Cube 8 flowcytometer, Sysmex Partec GmbH, Görlitz, Germany) by displaying cell counts (FL3-A, laser excitatory 488 nm, filter >670 nm) versus FSC-A (forward scatter) and SSC-A (side scatter), following to Almeida et al. (2019).

### 2.4.3. Pigment content

Aliquots of each culture (5 mL) were centrifuged at 5000g for 10 min. After removing most of the resulting supernatant (4 mL), the pellet was resuspended in the remaining supernatant and transferred to 2 mL microcentrifuge tubes for a second centrifugation (5000g for 5 min). The supernatant was discarded, and pellets were stored at  $-80^\circ\text{C}$  until further analysis. Pigments were extracted by resuspending the frozen pellets in 1 mL of solvent (80/20 acetone/methanol v/v) and incubating for 1 h at  $-20^\circ\text{C}$  in dark conditions. Ultrasonication was then performed on the solution at  $4^\circ\text{C}$  for 3 min, followed by incubation overnight at  $-20^\circ\text{C}$  to ensure total pigment extraction. Samples corresponding to weeks 1 to 4 and week 12, were analyzed by high-performance liquid chromatography (HPLC; Shimadze Prominence HPLC Systems). The extracts were then filtered through 0.45  $\mu$ m Target2™ Nylon Syringe 4 mm diameter Filters (Thermo Scientific™, cat n° F2504-1) and stored at  $-20^\circ\text{C}$  in dark glass vials until analyzed HPLC according to Corcoll et al. (2019). A total of 13 photosynthetic pigments were identified, including chlorophyllides (chlorophyll-*a*, chlorophyll-*b*, and pheophytin-*a*), carotenoids ( $\beta$ -carotene and  $\beta$ -E carotene) and xanthophylls (neoxanthin, violaxanthin, zeaxanthin, loraxanthin, lutein, 9-*cis* neoxanthin, antheraxanthin and canthaxanthin). Pigments were identified using internal standards, and relative abundance was estimated according to Wright and Jeffrey (2006).

Samples corresponding to weeks 9, 10 and 11 were analyzed by spectrophotometry. The extracts were centrifuged at 5000 rcf for 15 min to remove debris. 250  $\mu$ L of the supernatants were pipetted in 96 well-plates and immediately measured. The absorbance spectrum from 400 nm to 700 nm in 5 nm intervals was measured by a spectral scanning multimode reader (Varioskan Flash by Thermo Fisher Scientific).

The total carotenoids ( $C_{x+c}$ ) were calculated according to Wellburn (1994), using the equation:

$$C_{x+c} = (1000 A_{470} - 3,27C_a - 104C_b)/198$$

### 2.4.4. Photosynthetic quantum efficiency

The photosynthetic performance of cultures was determined from the quantum yield of photochemical energy conversion in PSII as measured after a saturation pulse (short pulse of 0.2 s) of red light (655 nm) using a Pulse Amplitude Modulated — PAM fluorometer (PhytoPAM-ED, Heinz Walz GmbH, Effeltrich, Germany). Samples of each culture (2 mL) were measured under agitation following a dark adaptation period of 15 min. Yield under quasi-dark-adapted conditions was calculated using the following equation:

$$\text{Yield} = \frac{dF}{F_m}$$

where  $F_m$  is the maximum fluorescence value and  $dF$  corresponds to the increase of fluorescence yield, from its current level ( $F = F_t$ ) to its maximum value ( $F_m$ ). The gain was adjusted for each measurement using the auto-gain function.

### 2.4.5. Tolerance tests

To compare the sensitivity of exposed and unexposed algae to diflufenican and to another environmental pollutant, viz. copper, algal ecotoxicological bioassays were performed according to the Organization for Economic Cooperation and Development (OECD) (Test No. 201, <http://www.oecd.org/>) guidelines and adjusted following Book et al. (2022). Starting cell density was set to ca. 20,000 cells/mL, and the algae were incubated for 72 h in 96 well plates under the same conditions as the main experiment. The working volume in each well was 200  $\mu$ L. Growth was measured using chlorophyll-*a* fluorescence values at time zero and after 72 h exposure using a fluorometer (VarioskanFlash version 4.00.53) at the excitation/emission wavelengths of 425 nm/680 nm. All assays were performed using one replicate from each treatment (i.e., replicate A) and were repeated at least twice, on weeks 9 and 10 after the start of the long-term experiment.

Each assay allowed ten test concentrations of toxicant, plus 30 controls, all of them performed in triplicates (Fig. S.1, Supplementary information plate layout). All outer wells of the 96-well plates were used as blanks since they showed a higher evaporation rate due to increased air exchange.

Diflufenican test concentrations were prepared in two steps. The same stock solution of 27.5 mg/L as the one used for the long-term exposure was first diluted to 3.6  $\mu$ g/L and a volume of 150  $\mu$ L was added to each of the wells in positions B2-D2. A 3.47-fold dilution series was performed directly in the plate, resulting in ten test concentrations ranging from 0.2 to 2.6  $\mu$ g/L. Finally, 50  $\mu$ L of algal suspension was added to each well and resuspended for mixing, resulting in a total volume of 200  $\mu$ L per well.

Copper chloride test concentrations were constructed in a similar way. A working stock concentration of 0.2 g/L of copper (II) chloride dihydrate (Sigma-Aldrich, 459097, CAS: 10125-13-0) was prepared in medium C, and a volume of 150  $\mu$ L was added to each of the wells in positions B2-D2. A 2.78-fold dilution series was performed directly in the plate, resulting in 10 test concentrations ranging from 0.02 to 230 mg/L. 50  $\mu$ L of algal suspension was added to each well, resulting in a total volume of 200  $\mu$ L per well.

The 72 h  $EC_{50}$  values were calculated based on the % inhibition of the growth rate (72 h  $EC_{50}$ ) compared to the control. The inhibition percentages were plotted against the test concentrations and the sigmoidal concentration-effect relationship was fitted to the Weibull model through the data points using the packages “tidyverse”, “drc”, and “readxl” in R v. 4.1. From this relationship, the 72 h  $EC_{50}$  values and their corresponding lower and upper limits (95 % confidence intervals) were derived. No overlapping between the confidence intervals were interpreted as significant differences between the compared  $EC_{50}$ s.

### 2.4.6. Fatty acid composition

Aliquots of each culture (10 mL) were filtered on 47-mm Whatman GF/F filters, immediately frozen in liquid nitrogen, and stored at  $-80^\circ\text{C}$  until further analysis. Fatty acid extractions were performed according to



Stamenković et al. (2019). Fatty acids were converted to fatty acid methyl esters (FAMES) by direct alkaline transmethylation and subjected to analysis on a GC–MS instrument (an Agilent 7820 gas chromatograph coupled to an Agilent 5975 mass selective detector, Agilent Technologies, USA). Data are expressed in pmol of total fatty acids per cell (Fig. 2a), and the fatty acids profiles are shown in relative abundance (molar proportion, mol%) (Fig. S.2, Supplementary information).

## 2.5. Diflufenican analysis

The media from all algal cultures (control and both diflufenican exposures) was sampled during week 1 and week 12, immediately after re-inoculation (t0h) and after 7 days afterwards. Briefly, 2 mL aliquots of each culture were centrifuged at 5000g for 20 min, with 1 mL of the resulting supernatant transferred to 1.5 mL dark glass vials (VWR international, vial scr. 1.5 mL, amber., 32 × 11.3 mm, cat n° 548-0448) and stored at –20 °C until further analysis. Water samples were analyzed by a 1200SL HPLC system (Agilent Technologies, Santa Clara, CA) coupled to an Agilent G6410A triple-quadrupole mass spectrometer (HPLC/MS/MS). Direct injection was performed after a 1:10 dilution and general source parameters for the Agilent 6410A were: for ES(+) : gas temperature 300 °C; gas flow 13 L/min; nebulizer 25 psi; capillary 4000 V; and for ES(–) : gas temperature 300 °C; gas flow 13 L/min; nebulizer 45 psi; and capillary 5000 V. Both Q1 and Q3 were set to unit resolution for all transitions. Diflufenican specific settings were set according to the method OMK 57:7 at the Swedish University of Agricultural Sciences (Uppsala, Sweden) following the protocol described by Jansson and Kreuger (2010). The whole system was controlled by MassHunter software for HPLC/MS/MS. The detection limit was 10 ng/L. Diflufenican was not detected in the control treatments. The analyzed diflufenican after medium renewal in the treatment of low concentration was  $10.7 \pm 0.2$  ng/L ( $n = 5$ ) and, in the treatment of higher concentration, was  $310.5 \pm 67$  ng/L ( $n = 5$ ) (Table S.1). Diflufenican concentrations declined to  $90 \pm 21.7$  ng/L ( $n = 3$ ) after 7 days of exposure due to abiotic losses of the compound in the test system.

## 2.6. Statistical analysis for phenotypic responses and diflufenican removal rate

Statistical differences in growth rate, photosynthetic yield, pigments content, fatty acids composition and diflufenican removal rate between exposed and non-exposed algae to the herbicide were assessed by one-way analysis of variance (ANOVA), followed by a Tukey post-hoc test for multiple comparisons. A post-hoc test with a  $p$ -value < 0.05 was considered statistically significant.

## 2.7. Transcriptome analysis via mRNA sequencing

### 2.7.1. RNA extraction

A volume of 10 mL of each culture was transferred into 50 mL sterile tubes and centrifuged at 1500g for 5 min, at 16 °C. After centrifugation, 9 mL of the supernatant was discarded, and the pellets resuspended in 1 mL of supernatant were transferred to 2 mL microcentrifuge tubes and centrifuged at 5000g for 5 min. The supernatant was removed, immediately frozen in liquid nitrogen, and then stored at –80 °C until RNA extraction (within 3 months). Extraction was performed using the PureLink™ RNA Mini Kit (Thermo Fisher Scientific, Waltham, MA, USA) following the manufacturer's instructions, with DNA contamination removed using PureLink™ DNase Set (Thermo Fisher Scientific, Waltham, MA, USA). Insufficient RNA was obtained for the samples belonging to the treatment 10 ng/L diflufenican for further sequencing analysis. Samples corresponding to controls ( $n = 3$ ) and test concentration 310 ng/L ( $n = 3$ ) were used for mRNA sequencing.

### 2.7.2. Sequencing

The integrity of the RNA samples was assessed using a 2100 Bioanalyzer (Agilent), obtaining a RQN (RNA quality number) value between 5.2 and 7.2. One sequencing library from each of the total RNA samples was

prepared using the TruSeq stranded mRNA library preparation kit with polyA selection (Illumina Inc.). Cluster generation and 150 cycles of paired-end sequencing of the six libraries fitted in one lane of an SP flowcell using the NovaSeq 6000 system and v1.5 sequencing chemistry (Illumina Inc.) were performed by the SNP&SEQ Technology Platform from the National Genomics Infrastructure (NGI) in Uppsala, Sweden. Each sample generated at least 1.6 M reads.

### 2.7.3. RNAseq data analysis

Paired-end, 150 bp long raw reads in FastQ format were evaluated using FastQC v 0.11.9 (<https://www.bioinformatics.babraham.ac.uk/projects/fastqc/>). Reads were trimmed for quality and adaptor contamination using BBDuk v 38.90 (<https://github.com/BioInfoTools/BBMap/blob/master/sh/bbdduk.sh>) with the following parameters: ref = truseq\_rna.fa. gz qtrim = f ktrim = r k = 20 min k = 11 h dist = 2 trimpolyg = 10 tpe tbo.

Trimmed reads were aligned to the reference genome *Raphidocelis subcapitata* 1.0 (GCA-003203535.1) using the Rsubread package v 2.10.4 (Liao et al., 2019), with an average genome of 65 % coverage. The analysis was followed by the estimation of read counts for each gene using the function featureCounts from Rsubreadpackage v 2.10.4 (Liao et al., 2014). Based on the count matrix, samples were clustered using principal component analysis (PCA), and differentially expressed genes (DEGs) were identified using the DESeq2 v 1.36.0 package, from Bioconductor v 3.15 (<https://bioconductor.org/packages/release/bioc/html/DESeq2.html>). The resulting  $p$ -values were adjusted using the Benjamini-Hochberg false discovery rate (FDR) algorithm. DEGs in acclimated algae relative to controls were identified with a cut-off of  $|\log_2 \text{Fold Change (FC)}| > 2$  and adj  $p$  value < 0.05. For visualization of DEGs, a volcano plot was constructed using the EnhancedVolcano (v 1.14) R package from Bioconductor (v 3.15).

Gene Ontology (GO) terms were assessed to the annotated *R. subcapitata* genome based on Ensembl annotation of the algal species *Chlamydomonas reinhardtii* (Chlamydomonadaceae). Gene set enrichment analysis was performed using the piano v 2.12 R package in Bioconductor. Fisher, Stouffer, and tail-strength tests were individually performed using as input the DEGs obtained from DESeq2. Their corresponding  $\log_2$  fold change adjusted  $p$ -values (calculated using the Benjamini-Hochberg FDR algorithm), and the GO terms individually associated with each gene were used to designate gene sets. The results from the tests performed individually were combined using the consensusHeatmap option, obtaining consensus scores that indicate the mean rank for each gene set by the different performed tests. A heatmap with the gene set consensus scores was created using the same option. The raw data were deposited to the NCBI short read archive (SRA) with BioProject accession number PRJNA908764 (<https://www.ncbi.nlm.nih.gov/sra/PRJNA908764>).

The significance of the upregulation of the carotenoid biosynthesis pathway was assessed by performing a permutation test. A score was created based on the sum of the  $\log_2$  fold-changes of the eight genes identified for this pathway. When a gene was identified in duplicate, the score that drove in a higher magnitude the direction of the gene was selected. A  $p$ -value was derived by comparing the observed score to a null distribution with scores calculated from randomly selected genes. The null distribution was generated from 10,000 scores and a  $p$ -value < 0.05 was considered statistically significant.

## 3. Results

### 3.1. Initial decrease and subsequent recovery on algal growth rate, photosystem II efficiency, and carotenoid pigments

During the first week of diflufenican exposure, algal growth rate was inhibited in a dose-response-dependent manner. The growth rate decreased by 12 % compared to the controls for algae exposed to 10 ng/L of the herbicide, corresponding to the 10 % effect concentration, EC<sub>10</sub> (Fig. 1a). Growth of algae exposed to 310 ng/L was inhibited by up to 55 % compared to the controls (Fig. 1a), suggesting that the spiked concentration of

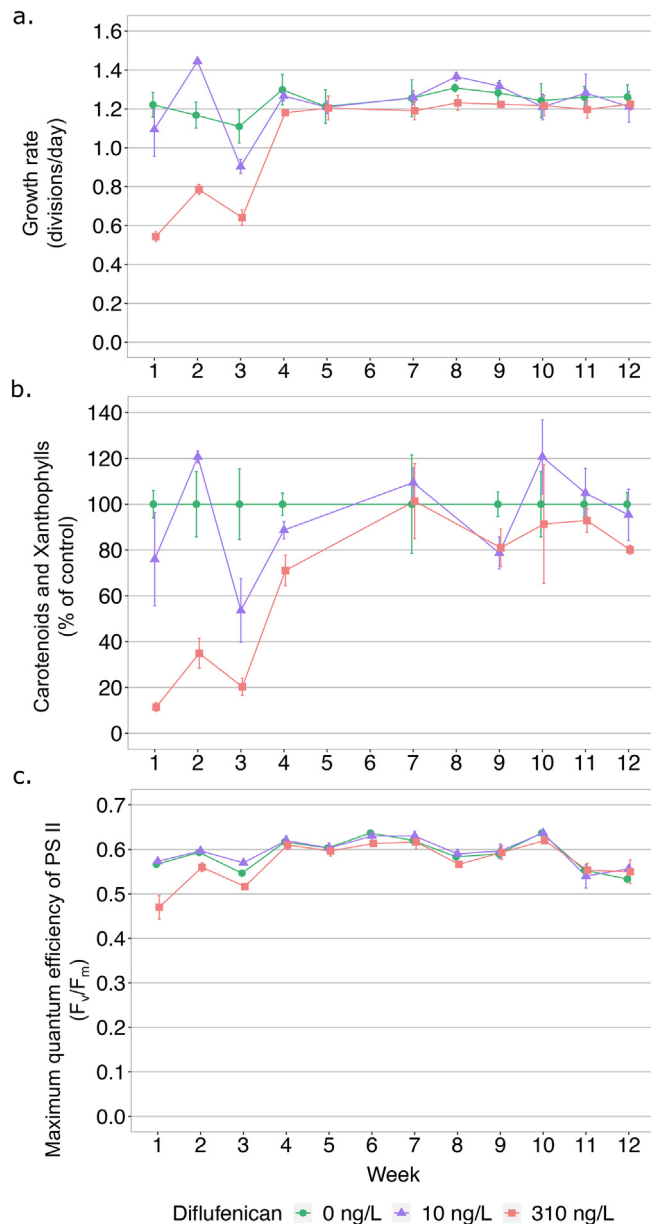


**Fig. 1.** Changes in *R. subcapitata* during the 12 weeks of the experiment in terms of growth rate after 3 days ( $\mu_{3\text{days}}$ ) of re-inoculation of new medium (a), relative carotenoids and xanthophyll content in relation to the control (b), and maximum quantum yield of photochemical energy conversion in PSII (c) when were exposed to 0 ng/L (●) 10 ng/L (▲), and 310 ng/L (■) of diflufenican. Figure shows mean and standard deviation of the three replicates per treatment.

diflufenican (310 ng/L) was near to the  $EC_{50}$  of the compound after 3 days of exposure. This initial decrease in growth was defined in our study as the stress phase, during which more pronounced changes were observed in the content of xanthophylls and carotenoids, with a decrease of down to a 22 % in algae exposed to 10 ng/L and up to 88 % in algae exposed to 310 ng/L compared to the controls (Fig. 1b). Effects on PSII photosynthetic activity during the stress phase were less pronounced (up to 17 %) and were only detected in algae exposed to 310 ng/L (Fig. 1c). After the stress phase (week 1), a gradual recovery of the growth rate, pigment content, and photosynthetic efficiency was noted during a period of two weeks. The growth rate, carotenoids and xanthophyll and photosynthetic activity of exposed algae to diflufenican returned to initial conditions and remained stable until the end of the experiment, showing little difference to the controls (Fig. 1a and c). This phase (from week 4 to week 12) was defined in our study as the acclimation phase.

### 3.2. Characterization of the acclimation phase at the end of the experiment

#### 3.2.1. Fatty acids, cell size, and tolerance induction

Total fatty acids content (Fig. 2a) and fatty acids profiles (Fig. 2.S, Supplementary information) were similar across all treatments in the acclimation phase ( $p\text{-adj} = 0.07$ , ANOVA post-hoc test). Furthermore, the acclimated algae had a smaller cell size, and this effect followed a dose-response manner. Algae acclimated to 10 or 310 ng/L of diflufenican were 5 or 13 % smaller in size compared to the control algae, respectively (Fig. 2b). Algae acclimated to 10 ng/L of diflufenican were also more tolerant to the herbicide with an  $EC_{50}$  (on growth rate) of 502 ng/L (Fig. 3a), which was 1.3 times higher than the  $EC_{50}$  in the control populations ( $EC_{50} 72 \text{ h} = 397 \text{ ng/L}$ ). Similarly, algae exposed to 310 ng/L of diflufenican exhibited an even higher tolerance to this compound, resulting in an  $EC_{50}$  of 965 ng/L, 2.4 times higher than the tested  $EC_{50}$  for the control populations (Fig. 3a). Acclimated algae were also exposed to copper to test for possible co-tolerance mechanisms. Interestingly, short-term exposure to copper revealed that algae acclimated to 10 or 310 ng/L of diflufenican did not have a higher capacity to tolerate copper than control populations (Fig. 3b). The reported  $EC_{50} 72 \text{ h}$  for the three treatments were 275.6  $\mu\text{g/L}$  for the control populations, 346.4  $\mu\text{g/L}$  in algae exposed to 10 ng/L and 284.74  $\mu\text{g/L}$  in algal populations acclimated to 310 ng/L.

#### 3.2.2. Change in transcription levels

Out of 11,581 genes analyzed for changes in transcription resulting from high diflufenican exposure, 156 (1.3 %) were differentially expressed in acclimated algae compared to the controls (using a strict cutoff of  $|\log_2 \text{Fold Change (FC)}| > 2$  and  $\text{adj } p \text{ value} < 0.05$ , Fig. 4). Of the 156 differentially expressed genes (DEGs), 148 were up-regulated and 8 down-regulated (Fig. 4). The up-regulated genes were mostly related functionally to cellular structure (e.g., tubulins), DNA synthesis and repair (e.g., ribonucleoside-diphosphate reductase and histones), global cell metabolism (e.g., kinases), cell transport (e.g., kinesins), and cell and plastid division (e.g., cyclins) (Fig. 4). In contrast, the down-regulated genes were all annotated as hypothetical proteins; and therefore, no functional insights could be ascertained (Table S.2).

Due to the mode of action of diflufenican, we also examined the expression levels of eight genes related to the carotenoid biosynthesis pathway. Although these genes individually showed no significant differential expression between the different treatments, we analyzed the overall expression pattern of the group of eight genes via a permutation test, to search for possible tendencies associated with the diflufenican exposure. This showed a significant ( $p = 0.042$ ) upregulation of genes downstream of Phytoene desaturase (PDS), and a downregulation of genes upstream of PDS, fitting into the classical negative/positive feedback pathway regulation (Fig. 5).

#### 3.2.3. Gene enrichment analysis based on gene ontology terms

In order to explore the role of the DEG in terms of molecular function, biological processes, and cellular component, a gene enrichment analysis based on GO terms was performed. The results are shown as a heatmap (Fig. 6) that illustrates the gene set consensus scores and the level of enrichment of each gene set according to a color scale. In total, 52 gene sets were differentially up-regulated, and 46 gene sets were down-regulated. Gene sets related to the functions of the DEGs were observed, notably up-regulation of the mitotic cell cycle, DNA repair and division, and cytoskeleton organization. Furthermore, up-regulation of gene sets related to protein folding, molecular chaperones, and heat shock proteins, hint the remaining stress of acclimated cells due to the presence of diflufenican (Fig. 6). Down-regulated gene sets were related to transcription and translation processes, including RNA polymerase complexes, cytoplasmic translation initiation complex, and ribosome biogenesis.

## 4. Discussion

In this study we investigated the changes in phenotype (i.e. physiological traits) and transcriptomics (i.e. gene expression) in the green microalgal

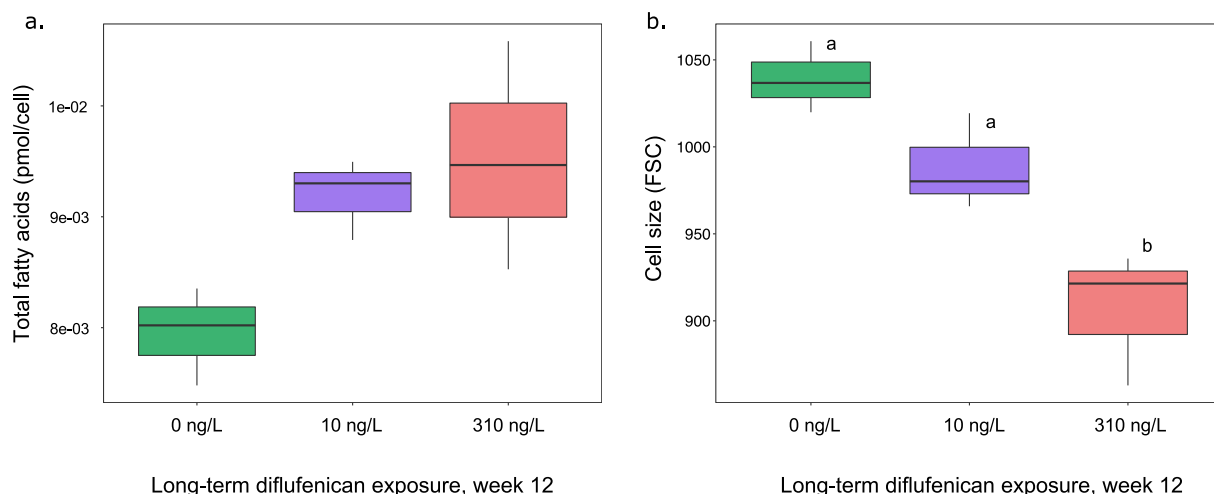


**Fig. 2.** Total fatty acids (pmol/cell) (a) and cell size (Forward scatter; FSC) (b) in *R. subcapitata* exposed to 0 ng/L of diflufenican (green boxes), 10 ng/L (purple boxes) and 310 ng/L (red boxes) for 12 weeks. The center line represents the median value (50th percentile), while the box contains the 25th to 75th percentiles of the dataset. The lines denote the 5 and 95th percentiles, and letters that are the same denote non-significant difference between results after using Tukey's test, meanwhile different letters denote significantly different results. (For interpretation of the references to color in this figure legend, the reader is referred to the web version of this article.)

model species *R. subcapitata* during acclimation to the herbicide diflufenican, a carotenoid biosynthesis inhibitor, when exposed for 12 weeks to two environmentally-relevant concentrations of 10 and 310 ng/L of diflufenican. In summary, an acclimation phase was achieved after a stress phase (first four weeks of exposure). The monitoring of growth, pigment composition and photosynthetic quantum yield through

the entire experiment revealed an initial stress phase followed by recovery and later acclimation of *R. subcapitata* towards the herbicide. In our study, acclimation was interpreted as the recovery and maintenance of growth rate levels similar to those of the non-exposed populations. Algae acclimated to 10 and 310 ng/L of diflufenican after 12 weeks of continuous

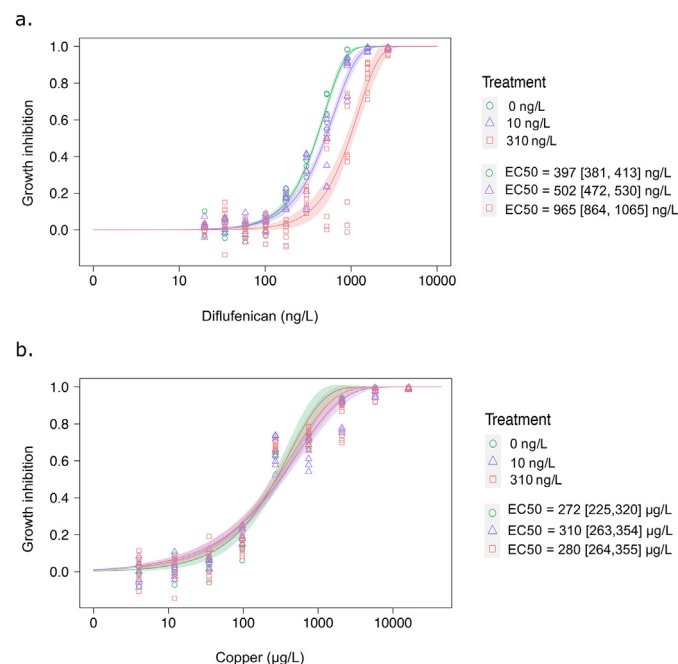


**Fig. 3.** Diflufenican (a) and copper chloride ( $\text{CuCl}_2$ ) (b) 72 h dose-response curves for *R. subcapitata* unexposed (green circles), acclimated to 10 ng/L (violet triangles), and to 310 ng/L of diflufenican (red squares) at the end of the experiment. The effect is calculated as relative inhibition of cell growth on a scale from 0 to 1 (0 to 100 % inhibition). Upper and lower  $\text{EC}_{50}$  values from 95 % confidence intervals are plotted and presented in brackets, next to the  $\text{EC}_{50}$  values. Tests for each long-term treatment were performed twice (weeks 9 and week 10), and each test contained three replicates. Modelling of dose-response curves and 50 % effect concentration ( $\text{EC}_{50}$ ) were estimated using the two-parameter model Weibull in R v. 4.2.1. (For interpretation of the references to color in this figure legend, the reader is referred to the web version of this article.)

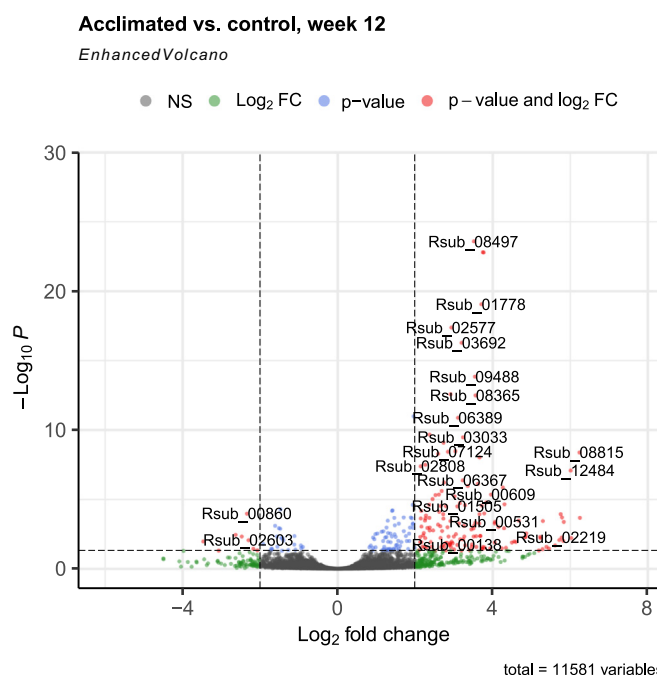


**Fig. 4.** Volcano plot comparison of gene expression in *R. subcapitata* after 80 d of exposure to 0 ng/L diflufenican (control) and 310 ng/L of diflufenican (week 12). The x axis indicates the differential expression profile at the gene level in a log-2 scale. The y axis indicates the statistical significance of the difference in expression (adjusted  $p$  value from DeSeq2) in a log10 scale. Each dot represents a gene. Differentially expressed genes with a log 2 fold change (FC) higher than |2| and adjusted  $p$ -value lower than 0.05, are shown in red ( $p$ -value and  $\text{Log}_2$  FC). Non-significant genes are shown in light-gray dots (NS), and genes with a log 2 fold change higher than |2|, but adjusted  $p$ -value higher than 0.05 are shown in green ( $\text{Log}_2$  FC). Genes with log 2 fold change lower than |2|, and  $p$ -value lower than 0.05 are represented in blue. (For interpretation of the references to color in this figure legend, the reader is referred to the web version of this article.)

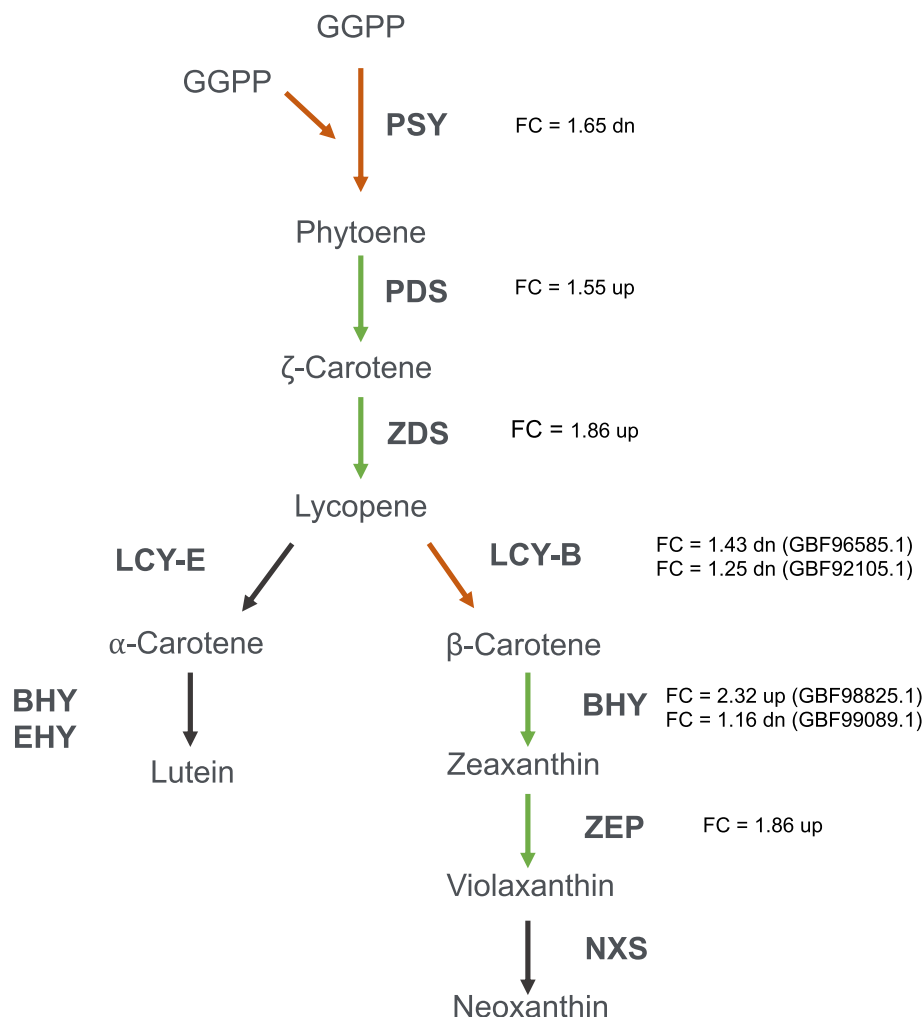


**Fig. 5.** Scheme of the carotenoid biosynthesis pathway and main enzymes up- or down-regulated in *R. subcapitata* after 80 d of exposure to 310 ng/L of diflufenican in comparison to non-exposed algae (0 ng/L diflufenican). Up-regulated genes coding for enzymes involved in the reaction steps according to the differential expression analysis performed are marked in green arrows, and down-regulated genes are marked in red arrows. The stated fold-change (FC) indicated for each enzyme is obtained from DeSeq2 analysis (Wald test). The group of eight genes represented in the figure was subjected to a permutation test ( $n = 10,000$ ;  $p = 0.04$ ), which showed that the pathway was significantly upregulated downstream the target enzyme (PDS) and a downregulated upstream carotenoid biosynthesis pathway. Abbreviations: GGPP, geranylgeranyl diphosphate; PSY, phytoene synthase; PDS, phytoene desaturase; ZDS, zeta-carotene desaturase; LCY-B, lycopene beta cyclase; LCY-E, lycopene epsilon cyclase; BHY, beta-carotene hydroxylase; EHY, epsilon carotene hydroxylase; ZEP, zeaxanthin epoxidase; NXS, neoxanthin synthase. (For interpretation of the references to color in this figure legend, the reader is referred to the web version of this article.)

exposure were increasingly more tolerant to diflufenican (1.3 and 2.4 times, respectively) than non-exposed algae. However, algae acclimated to 310 ng/L did not recover their initial cell size to their initial values.

The mode of action of diflufenican is well documented (Böger, 1996; Dang et al., 2019; Feckler et al., 2018), and it has proven to be effective in significantly lowering the synthesis of carotenoids (Miras-Moreno et al., 2019). Therefore, the initial recovery (week 7) and subsequent maintenance of 80 % (weeks 9–12) of carotenoid content after three months of continuous exposure to concentrations of diflufenican close to  $EC_{50}$  values should be interpreted as an indication of the phenotypic plasticity of *R. subcapitata* rather than as an inability to fully restore all values to the initial states. Along the same line, even though the individual expression of the genes involved in the carotenoid biosynthesis pathway was not significant, the overall tendency of the pathway showed an upregulation downstream the target enzyme (PDS), and a downregulation upstream, fitting into the classical negative/positive feedback pathway regulation, allowing an active maintenance of carotenoid biosynthetic pathway in acclimated algae.

The acclimated algae were also assessed for fatty acids profile, diflufenican removal rate, and cell size. Previous studies have found that microalgae are able to bioaccumulate a wide range of chemicals

(Abdelfattah et al., 2022; Kim et al., 2019; Leong and Chang, 2020). Bioaccumulation has also been linked to changes in fatty acids, such as in one study describing how algae exposed to high concentrations of atrazine showed a decrease in their total fatty acid content and shift in fatty acid composition (Kabra et al., 2014). Moreover, it has been described that variations in total fatty acid content or the percentage of a given fatty acid class may be indicative of a pesticide interfering with the normal metabolism of an organism (Gonçalves et al., 2021). However, our results indicated that algal fatty acid composition and total content of fatty acids were unaffected by the herbicide.

Genes related to bioaccumulation or biodegradation in microalgae such as oxidative stress-related genes, oxidases or hydrolases (Bi et al., 2012; Zhao et al., 2021) were not differentially expressed in our study (Table S.2), leaving us to hypothesize that *R. subcapitata* is able to cope with high concentrations of diflufenican without accumulating or using the herbicide as a source of energy.

Acclimated algae to diflufenican were smaller in size. Because acclimation processes and coping with an environmental stressor increase the demand for resources ( $O_2$ ,  $CO_2$ , and nutrients), microalgae can reduce their cell size to surface area in order to enhance uptake of nutrients and reduce



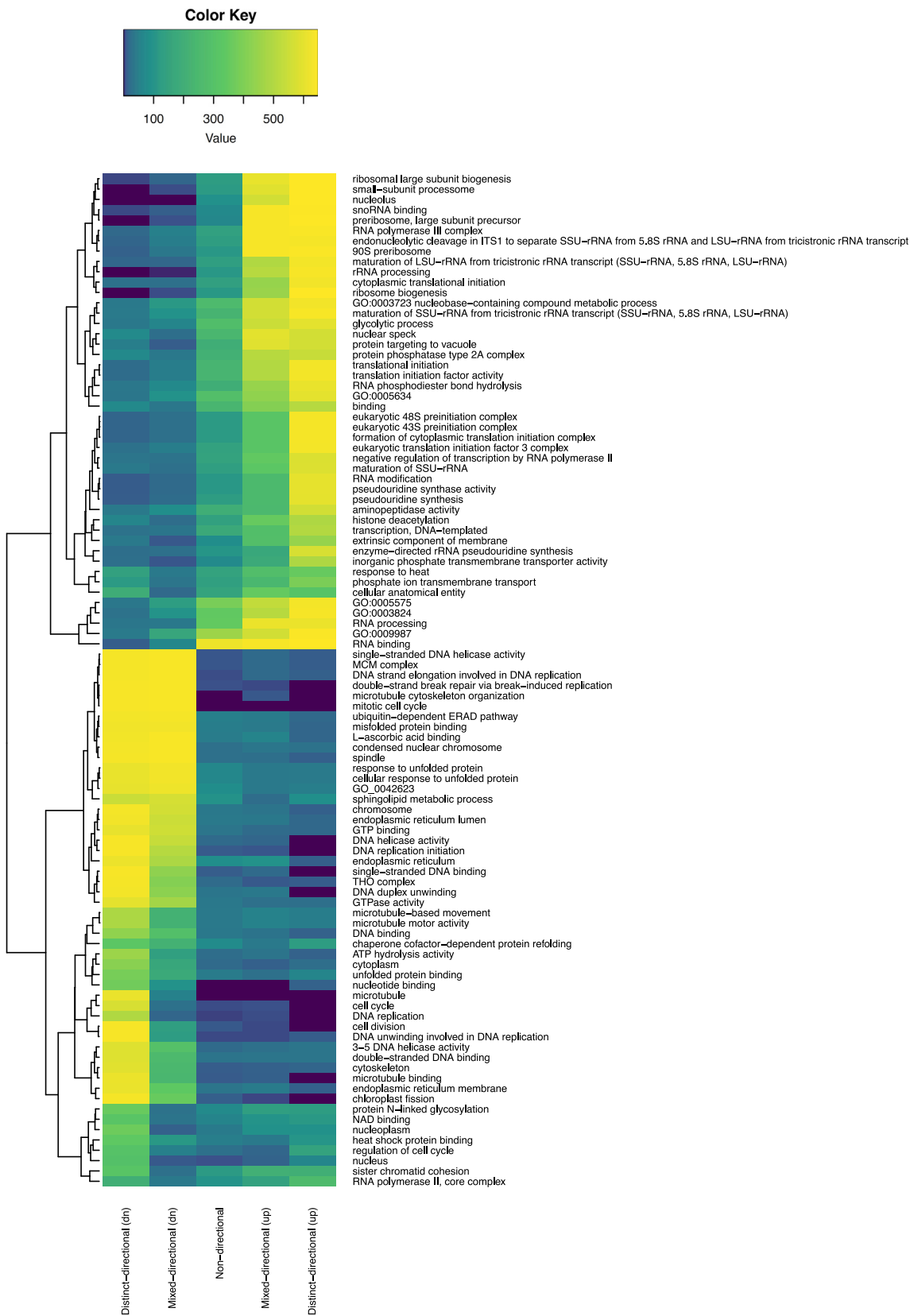


**Fig. 6.** Heatmap of the gene set consensus scores of the top-ranked gene sets for each of the directionality classes. The consensus score is the mean rank assigned to each gene set by Fisher, Stouffer, and tail-strength tests, meaning that a low score (e.g., 1) is a gene set that is ranked high by most of the GSA methods. The score corresponds to the shown color scale. The non-directional class disregards the fold change of the gene set and instead uses the absolute values of the gene-level statistics to calculate the gene set statistics and the associated *p*-values. The distinct-directional class takes fold changes of each gene into account, so that gene sets with genes both significantly up-regulated and significantly down-regulated will cancel out. The mixed-directional class considers the up-regulated subset and the down-regulated subset of a gene set separately.

metabolic costs (Staehr and Birkeland, 2006). Changing environmental conditions can result in a loss of equilibrium between energy flux provided by photosynthesis and the synthesis of macromolecules, leading to changes in nutrient acquisition, defense mechanisms, stress-induced repair activities, and/or cell cycle activity (Wagner et al., 2017; Wilhelm and Jakob, 2011). In our study, gene sets related to the cellular structure were found to be upregulated, as were genes related to cellular division, DNA repair and replication, and protein folding. This general response might be due to differences in carbon allocation with the purpose of maintaining a stable cellular growth. Previous studies have reported that the acclimation of different microalgal species to wastewater, high-dose phenols and levofloxacin have induced an increase in microalgal growth (Cho et al., 2016; Osudenko, 2014; Xiong et al., 2017).

The enzyme zeaxanthin epoxidase (ZEP) showed a tendency – even though not significant by itself, but as pathway – of being up-regulated in acclimated algae. It can be hypothesized that acclimated algae could be experiencing a dysregulation of the cellular cycle due to the potential lack of abscisic acid (ABA), one of the main phytohormones. Although the function of ABA in terrestrial plants has been characterized in detail (Rai et al., 2011), its function in microalgae remains poorly understood. In eukaryotic algae, ABA has been associated with the regulation of the cell cycle and stress resistance (Hartung, 2010; Nagamune et al., 2008; Tuteja, 2007; Yoshida et al., 2004). ABA activates the expression of the heme-scavenger TSP0 protein, which prevents the cell cycle G1/S progression (Kobayashi et al., 2016). Interestingly, the first stage of the direct pathway of ABA biosynthesis is the synthesis of carotenoids. The first reaction assumed to be essential for ABA synthesis is the conversion of zeaxanthin into trans-violaxanthin via two-step de-epoxidation, catalyzed by ZEP (Kiseleva et al., 2012). Therefore, it is possible that under a scenario of reduced carotenoid synthesis — stress phase, a consequent drop in ABA concentration could accelerate the G1/S progression in the cell cycle, resulting in -acclimation phase- an up-regulation of the genes related to the carotenoid biosynthesis pathway, faster organelle and cell division, increased DNA replication and damage, and protein misfolding, together with a smaller cell size.

## 5. Conclusions

This study demonstrates the significant phenotypic plasticity of *R. subcapitata* to acclimate to environmental but toxic levels of diflufenican and in turn the trade-off expenses of tolerance development via changes in gene expression, and reduction of cell size. The transcriptome profiling suggested a fitness cost to acclimation, by revealing a residual stress state that implies a degree of protein damage and translational impairment, protein unfolding, and DNA repair and malfunctioning of the cell cycle. According to the observed effects, the environmental risk of herbicides in freshwater ecosystems remains high, and further studies would be needed to assess how acclimation would work in a situation of global change in which multiple stressors (i.e., light, temperature, other pollutants) are co-occurring or how acquired acclimation mechanism will react once the stressor ceases.

Supplementary data to this article can be found online at <https://doi.org/10.1016/j.scitotenv.2023.162604>.

## CRedit authorship contribution statement

Daniela Gómez-Martínez: Conceptualization, Methodology, Investigation, Formal analysis, Data curation, Writing – original draft, Writing-review & editing. Johanna Bengtson: Investigation, Writing – review & editing. Anders K. Nilsson: Investigation, Writing – review & editing. Adrian K. Clarke: Methodology, Writing – review & editing. Rolf Henrik Nilsson: Methodology, Writing – review & editing. Erik Kristiansson: Methodology, Data curation, Supervising – bioinformatics, Writing – review & editing. Natàlia Corcoll: Conceptualization, Methodology, Investigation, Formal analysis, Data curation, Supervision – whole project, Writing – review & editing. Funding acquisition.

## Data availability

Data will be made available on request.

## Declaration of competing interest

The authors declare that they have no known competing financial interests or personal relationships that could have appeared to influence the work reported in this paper.

## Acknowledgments

This study was financed by the Swedish Research Council Formas project “HERBEVOL”(grant no. 2015-1464) and the Swedish Foundation Stiftelsen Brigit och Birger Wählströms minnesfond för den Bohuslänska havs-och insjömiljön. EK gratefully acknowledges funding from the Center for Future Chemical Risk Assessment and Management Strategies (FRAM) at the University of Gothenburg. Diflufenican analyses were performed by the Swedish University of Agriculture (SLU) in Uppsala. Sequencing was performed by the SNP&SEQ Technology Platform in Uppsala. The facility is part of the National Genomics Infrastructure (NGI) Sweden and Science for Life Laboratory. The SNP&SEQ Platform is also supported by the Swedish Research Council and the Knut and Alice Wallenberg Foundation.

## References

- Abdelfattah, A., Ali, S.S., Ramadan, H., El-Aswar, E.I., Eltabaw, R., Ho, S.-H., Elsamahy, T., Li, S., El-Sheekh, M.M., Schagerl, M., Kornaros, M., Sun, J., 2022. Microalgae-based wastewater treatment: mechanisms, challenges, recent advances, and future prospects. *Environ. Sci. Ecotechnol.* 13, 100205. <https://doi.org/10.1016/j.ese.2022.100205>.
- Almeida, A.C., Gomes, T., Habuda-Stanić, M., Lomba, J.A.B., Romić, Ž., Turkalj, J.V., Lillcrap, A., 2019. Characterization of multiple biomarker responses using flow cytometry to improve environmental hazard assessment with the green microalgae *raphidocelis subcapitata*. *Sci. Total Environ.* 687, 827–838. <https://doi.org/10.1016/j.scitotenv.2019.06.124>.
- Bi, Y.F., Miao, S.S., Lu, Y.C., Qiu, C.B., Zhou, Y., Yang, H., 2012. Phytotoxicity, bioaccumulation and degradation of isoproturon in green algae. *J. Hazard. Mater.* 243, 242–249. <https://doi.org/10.1016/j.jhazmat.2012.10.021>.
- Böger, P., 1996. Mode of action of herbicides affecting carotenogenesis. *J. Pest. Sci.* 21 (4), 473–478. <https://doi.org/10.1584/jpestics.21.473>.
- Book, F., Persson, M., Carmona, E., Backhaus, T., Lammel, T., 2022. Colloidal silica nanomaterials reduce the toxicity of pesticides to algae, depending on charge and surface area. *Environ. Sci. Nano* 9 (7), 2402–2416. <https://doi.org/10.1039/d1en01180d>.
- Boström, G., Gönczi, M., Kreuger, J., 2017. Växtskyddsmedel som regelbundet överskrider riktvärden för ytvatten – en undersökning av bakomliggande orsaker. Centre for Chemical Pesticides. Swedish University of Agricultural Science.
- Boye, K., Lindström, B., Boström, G., Kreuger, J., 2019. Long-term data from the Swedish National Environmental Monitoring Program of pesticides in surface waters. *J. Environ. Qual.* 48 (4), 1109–1119. <https://doi.org/10.2134/jeq2019.02.0056>.
- Ceschin, S., Bellini, A., Scalici, M., 2021. Aquatic plants and ecotoxicological assessment in freshwater ecosystems: a review. *Environ. Sci. Pollut. Res.* 28 (5), 4975–4988. <https://doi.org/10.1007/s11356-020-11496-3>.
- Chalifour, A., Tam, N.F.Y., 2016. Tolerance of cyanobacteria to the toxicity of BDE-47 and their removal ability. *Chemosphere* 164, 451–461. <https://doi.org/10.1016/j.chemosphere.2016.08.109>.
- Cho, K., Lee, C.H., Ko, K., Lee, Y.J., Kim, K.N., Kim, M.K., Chung, Y.H., Kim, D., Yeo, I.K., Oda, T., 2016. Use of phenol-induced oxidative stress acclimation to stimulate cell growth and biodiesel production by the oceanic microalga *Dunaliella Salina*. *Algal Res.* 17, 61–66. <https://doi.org/10.1016/j.algal.2016.04.023>.
- Corcoll, N., Yang, J., Backhaus, T., Zhang, X., Eriksson, K.M., 2019. Copper affects composition and functioning of microbial communities in marine biofilms at environmentally relevant concentrations. *Front. Microbiol.* 10 (JAN), 1–15. <https://doi.org/10.3389/fmicb.2018.03248>.
- Dang, H.T., Malone, J.M., Gill, G., Preston, C., 2019. Cross-resistance to diflufenican and picolinafen and its inheritance in oriental mustard (*Sisymbrium orientale* L.). *Pest Manag. Sci.* 75 (1), 195–203. <https://doi.org/10.1002/ps.5087>.
- Feckler, A., Rakovic, J., Kahlert, M., Tröger, R., Bundschuh, M., 2018. Blinded by the light: increased chlorophyll fluorescence of herbicide-exposed periphyton masks unfavorable structural responses during exposure and recovery. *Aquat. Toxicol.* 203 (August), 187–193. <https://doi.org/10.1016/j.aquatox.2018.08.015>.
- Gonçalves, A.M.M., Rocha, C.P., Marques, J.C., Gonçalves, F.J.M., 2021. Fatty acids as suitable biomarkers to assess pesticide impacts in freshwater biological scales – a review. *Ecol. Indic.* 122. <https://doi.org/10.1016/j.ecolind.2020.107299>.
- Hartung, W., 2010. The evolution of abscisic acid (ABA) and ABA function in lower plants, fungi and lichen. *Funct. Plant Biol.* 37 (9), 806–812. <https://doi.org/10.1071/FP10058>.
- Herrero-Hernández, E., Simón-Egea, A.B., Sánchez-Martín, M.J., Rodríguez-Cruz, M.S., Andrades, M.S., 2020. Monitoring and environmental risk assessment of pesticide residues and some of their degradation products in natural waters of the Spanish vineyard

- region included in the denomination of origin Jumilla. *Environ. Pollut.* 264. <https://doi.org/10.1016/j.envpol.2020.114666>.
- Huertas, I.E., Rouco, M., López-Rodas, V., Costas, E., 2010. Estimating the capability of different phytoplankton groups to adapt to contamination: herbicides will affect phytoplankton species differently. *New Phytol.* 188 (2), 478–487. <https://doi.org/10.1111/j.1469-8137.2010.03370.x>.
- Ichimura, T., 1971. Sexual cell division and conjugation-papilla formation in sexual reproduction of *Closterium strigosum*. *Proceedings of the 7th International Seaweed Symposium*, pp. 208–214.
- Jansson, C., Kreuger, J., 2010. Multiresidue analysis of 95 pesticides at low nanogram/liter levels in surface waters using online preconcentration and high performance liquid chromatography/tandem mass spectrometry. *J. AOAC Int.* 93 (6), 1732–1747. <https://doi.org/10.1093/jaoac/93.6.1732>.
- Kabra, A.N., Ji, M.K., Choi, J., Kim, J.R., Govindwar, S.P., Jeon, B.H., 2014. Toxicity of atrazine and its bioaccumulation and biodegradation in a green microalga, *Chlamydomonas mexicana*. *Environ. Sci. Pollut. Res.* 12270–12278. <https://doi.org/10.1007/s11356-014-3157-4>.
- Kim, I., Yang, H.M., Park, C.W., Yoon, I.H., Seo, B.K., Kim, E.K., Ryu, B.G., 2019. Removal of radioactive cesium from an aqueous solution via bioaccumulation by microalgae and magnetic separation. *Sci. Rep.* 9 (1), 3–10. <https://doi.org/10.1038/s41598-019-46586-x>.
- Kiseleva, A.A., Tarachovskaya, E.R., Shishova, M.F., 2012. Biosynthesis of phytohormones in algae. *Russ. J. Plant Physiol.* 59 (5), 595–610. <https://doi.org/10.1134/S1021443712050081>.
- Kobayashi, Y., Ando, H., Hanaoka, M., Tanaka, K., 2016. Absciscic acid participates in the control of cell cycle initiation through heme homeostasis in the unicellular red alga *Cyanidioschyzon merolae*. *Plant Cell Physiol.* 57 (5), 953–960. <https://doi.org/10.1093/pcp/pcw054>.
- LaPanse, A.J., Krishnan, A., Posewitz, M.C., 2021. Adaptive laboratory evolution for algal strain improvement: methodologies and applications. *Algal Res.* 53 (November 2020), 102122. <https://doi.org/10.1016/j.algal.2020.102122>.
- Leong, Y.K., Chang, J.S., 2020. Bioremediation of heavy metals using microalgae: recent advances and mechanisms. *Bioresour. Technol.* 303 (January), 122886. <https://doi.org/10.1016/j.biortech.2020.122886>.
- Liao, Y., Smyth, G.K., Shi, W., 2014. FeatureCounts: an efficient general purpose program for assigning sequence reads to genomic features. *Bioinformatics* 30 (7), 923–930. <https://doi.org/10.1093/bioinformatics/btt656>.
- Liao, Y., Smyth, G.K., Shi, W., 2019. The R package rsubread is easier, faster, cheaper and better for alignment and quantification of RNA sequencing reads. *Nucleic Acids Res.* 47 (8). <https://doi.org/10.1093/nar/gkz114>.
- Messelhäuser, M.H., Saile, M., Sievernich, B., Gerhards, R., 2021. Effect of cinmethylin against *Alopecurus myosuroides* huds. in winter cereals. *Plant Soil Environ.* 67 (1), 46–54. <https://doi.org/10.17221/586/2020-PSE>.
- Miras-Moreno, B., Pedreño, M.A., Fraser, P.D., Sabater-Jara, A.B., Almagro, L., 2019. Effect of diflufenican on total carotenoid and phytoene production in carrot suspension-cultured cells. *Planta* 249 (1), 113–122. <https://doi.org/10.1007/s00425-018-2966-y>.
- Nagamune, K., Hicks, L.M., Fux, B., Brossier, F., Chini, E.N., Sibley, L.D., 2008. Absciscic acid controls calcium-dependent egress and development in *Toxoplasma gondii*. *Nature* 451 (7175), 207–210. <https://doi.org/10.1038/nature06478>.
- Osundenko, O., 2014. A. Dean, H. Davies, J. Pittman, acclimation of microalgae to wastewater environments involves increase oxidative stress tolerance activity. *Plant Cell Physiol* 10, 1848–1857.
- Rai, M.K., Shekhawat, N.S., Harish, Gupta, A.K., Phulwaria, M., Ram, K., Jaiswal, U., 2011. The role of abscisic acid in plant tissue culture: a review of recent progress. *Plant Cell Tissue Organ Cult.* 106 (2), 179–190. <https://doi.org/10.1007/s11240-011-9923-9>.
- Ramaraj, R., Tsai, D.D.W., Chen, P.H., 2014. An exploration of the relationships between microalgae biomass growth and related environmental variables. *J. Photochem. Photobiol. B Biol.* 135, 44–47. <https://doi.org/10.1016/j.jphotobiol.2014.04.001>.
- Staehr, P.A., Birkeland, M.J., 2006. Temperature acclimation of growth, photosynthesis and respiration in two mesophilic phytoplankton species. *Phycologia* 45 (6), 648–656. <https://doi.org/10.2216/06-04.1>.
- Stamenković, M., Steinwall, E., Nilsson, A.K., Wulff, A., 2019. Desmids (Zygnemataphyceae, Streptophyta) as a promising freshwater microalgal group for the fatty acid production: results of a screening study. *J. Appl. Phycol.* 31 (2), 1021–1034. <https://doi.org/10.1007/s10811-018-1598-8>.
- Thiriet-Rupert, S., Gain, G., Jadoul, A., Vigneron, A., Bosman, B., Carnol, M., Motte, P., Cardol, P., Nouet, C., Hanikenne, M., 2021. Long-term acclimation to cadmium exposure reveals extensive phenotypic plasticity in *Chlamydomonas*. *Plant Physiol.* 187 (3), 1653–1678. <https://doi.org/10.1093/plphys/kiab375>.
- Tuteja, N., 2007. Absciscic acid and abiotic stress signaling. *Plant Signal. Behav.* 2 (3), 135–138. <https://doi.org/10.4161/psb.2.3.4156>.
- Wagner, H., Jakob, T., Fanesi, A., Wilhelm, C., 2017. Towards an understanding of the molecular regulation of carbon allocation in diatoms: the interaction of energy and carbon allocation. *Philos. Trans. R. Soc. B: Biol. Sci.* 372 (1728). <https://doi.org/10.1098/rstb.2016.0410>.
- Wellburn, A.R., 1994. The spectral determination of chlorophylls a and b, as well as total carotenoids, using various solvents with spectrophotometers of different resolution. *J. Plant Physiol.* 144 (3), 307–313. [https://doi.org/10.1016/S0176-1617\(11\)81192-2](https://doi.org/10.1016/S0176-1617(11)81192-2).
- Weyman, G.S., Rufli, H., Weltje, L., Salinas, E.R., Hamitou, M., 2012. Aquatic toxicity tests with substances that are poorly soluble in water and consequences for environmental risk assessment. *Environ. Toxicol. Chem.* 31 (7), 1662–1669. <https://doi.org/10.1002/etc.1856>.
- Wilhelm, C., Jakob, T., 2011. From photons to biomass and biofuels: evaluation of different strategies for the improvement of algal biotechnology based on comparative energy balances. *Appl. Microbiol. Biotechnol.* 92 (5), 909–919. <https://doi.org/10.1007/s00253-011-3627-2>.
- Wright, S.W., Jeffrey, S.W., 2006. In: Volkman, J.K. (Ed.), *Pigment Markers for Phytoplankton Production BT - Marine Organic Matter: Biomarkers, Isotopes and DNA*. Springer, Berlin Heidelberg, pp. 71–104. <https://doi.org/10.1007/978-2-003>.
- Wu, N., Dong, X., Liu, Y., Wang, C., Baattrup-Pedersen, A., Riis, T., 2017. Using river microalgae as indicators for freshwater biomonitoring: review of published research and future directions. *Ecol. Indic.* Vol. 81. Elsevier B.V., pp. 124–131. <https://doi.org/10.1016/j.ecolind.2017.05.066>.
- Xiong, J.Q., Kurade, M.B., Jeon, B.H., 2017. Biodegradation of levofloxacin by an acclimated freshwater microalga, *Chlorella vulgaris*. *Chem. Eng. J.* 313, 1251–1257. <https://doi.org/10.1016/j.cej.2016.11.017>.
- Yoshida, T., Hairston, N.G., Ellner, S.P., 2004. Evolutionary trade-off between defence against grazing and competitive ability in a simple unicellular alga, *Chlorella vulgaris*. *Proc. R. Soc. B Biol. Sci.* 271 (1551), 1947–1953. <https://doi.org/10.1098/rspb.2004.2818>.
- Zhao, C.Y., Ru, S., Cui, P., Qi, X., Kurade, M.B., Patil, S.M., Jeon, B.H., Xiong, J.Q., 2021. Multiple metabolic pathways of enrofloxacin by *Lolium perenne* L.: ecotoxicity, biodegradation, and key driven genes. *Water Res.* 202 (May), 117413. <https://doi.org/10.1016/j.watres.2021.117413>.